Micellar Organization and Dynamics: A Wavelength-Selective Fluorescence Approach

Satinder S. Rawat, Sushmita Mukherjee,† and Amitabha Chattopadhyay*

Centre for Cellular & Molecular Biology, Uppal Road, Hyderabad 500 007, India

Received: September 9, 1996; In Final Form: November 26, 1996[⊗]

Wavelength-selective fluorescence comprises a set of approaches based on the red edge effect in fluorescence spectroscopy, which can be used to monitor directly the environment and dynamics around a fluorophore in a complex biological system. A shift in the wavelength of maximum fluorescence emission toward higher wavelengths, caused by a shift in the excitation wavelength toward the red edge of the absorption band, is termed the red edge excitation shift (REES). This effect is mostly observed with polar fluorophores in motionally restricted media such as very viscous solutions or condensed phases. We have previously shown that REES and related techniques (wavelength-selective fluorescence approach) offer a novel way to monitor organization and dynamics of membrane-bound probes and peptides. In this paper, we report REES of NBD-PE, a phospholipid whose headgroup is covalently labeled with the 7-nitrobenz-2-oxa-1,3-diazol-4-yl (NBD) moiety, when incorporated into micelles formed by a variety of detergents (SDS, Triton X-100, CTAB and CHAPS) which differ in their charge and organization. In addition, fluorescence polarization of NBD-PE in these micelles shows both excitation and emission wavelength dependence. The lifetime of NBD-PE was found to be dependent on both excitation and emission wavelengths. These wavelength-dependent lifetimes are correlated to the reorientation of solvent dipoles around the excited-state dipole of the NBD group in micellar environments. Taken together, these observations are indicative of the motional restriction experienced by the fluorophore when bound to micelles. Wavelength-selective fluorescence promises to be a powerful tool for studying micellar organization and dynamics.

Introduction

Detergents are soluble amphiphiles and above a critical concentration (strictly speaking, a narrow concentration range), known as the critical micelle concentration (cmc), self-associate to form thermodynamically stable, noncovalent aggregates called micelles.[1] The studies on micellar organization and dynamics assume special significance in light of the fact that the general principles underlying the formation of micelles are common to other related assemblies such as reverse micelles, bilayers, liposomes, and biological membranes.[1−4] Micelles have also been applied as membrane mimetics to characterize membrane proteins and peptides.[5−8] Further, micelles have been used as a model for the anesthetic action of certain pharmacological compounds[9] and for creating nanostructures.[10] The phenomenon of micellization also plays a vital role in the human digestive system where micelles formed by bile salts (which are detergents produced by the liver from cholesterol and secreted into the intestine) help solubilize the fat ingested as part of the diet.[11]

Micelles are highly cooperative, organized molecular assemblies of amphiphiles and are dynamic in nature.[12,13] A direct consequence of such organized systems is the restriction imposed on the dynamics and mobility of their constituent structural units. We have previously shown that the microenvironment of molecules bound to such organized assemblies can be conveniently monitored using wavelength-selective fluorescence as a novel tool.[14−19] Wavelength-selective fluorescence comprises a set of approaches based on the red edge effect in fluorescence spectroscopy, which can be used to monitor directly the environment and dynamics around a fluorophore in a complex biological system.[20] A shift in the wavelength of maximum fluorescence emission toward higher wavelengths, caused by a shift in the excitation wavelength toward the red edge of the absorption band, is termed the red edge excitation shift (REES). This effect is mostly observed with polar fluorophores in motionally restricted media such as very viscous solutions or condensed phases (refs 20 and 21 and references therein). This phenomenon arises from the slow rates of solvent relaxation (reorientation) around an excited-state fluorophore, which is a function of the motional restriction imposed on the solvent molecules in the immediate vicinity of the fluorophore. Utilizing this approach, it becomes possible to probe the mobility parameters of the environment itself (which is represented by the relaxing solvent molecules) using the fluorophore merely as a reporter group. Further, since the ubiquitous solvent for biological systems is water, the information obtained in such cases will come from the water molecules. This makes REES and related techniques extremely useful in biology since hydration plays a crucial modulatory role in a large number of important cellular events such as lipid−protein interactions[22] and ion transport.[23−25]

We have previously shown that REES and related techniques (wavelength-selective fluorescence approach) serve as a powerful tool to monitor organization and dynamics of membrane-bound probes and peptides. In one of our studies, the wavelength-selective fluorescence characteristics of the widely used membrane probe *N*-(7-nitrobenz-2-oxa-1,3-diazol-4-yl)-1,2-dipalmitoyl-*sn*-glycero-3-phosphoethanolamine (NBD-PE), when bound to model membranes of dioleoyl-*sn*-glycero-3-phosphocholine (DOPC), was reported.[15] We have also monitored the tryptophan environments in membrane-bound peptides such as melittin, a powerful hemolytic peptide from the venom of the honey bee *Apis mellifera*,[16,26] and in the channel forming peptide gramicidin, produced by the bacteria *Bacillus brevis*.[17]

† Present address: Room 15-420, Department of Pathology, College of Physicians and Surgeons, Columbia University, 630 West 168th Street, New York, NY 10032.

* Address correspondence to this author. E-mail: amitabha@ccmb.globemail.com.

⊗ Abstract published in *Advance ACS Abstracts,* February 1, 1997.

S1089-5647(96)02736-8 CCC: $14.00

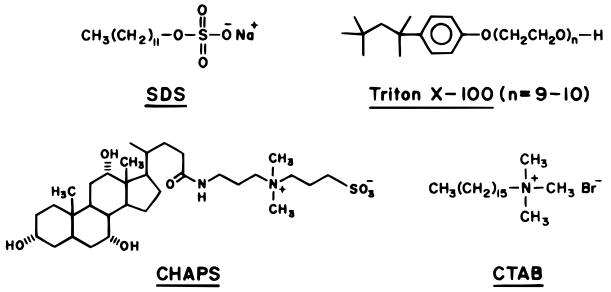

Figure 1. Chemical structures of detergents used.

Interestingly, in both these peptides the tryptophan residues have been shown to be extremely important for the function of the peptide.[27,28]

Micelles represent yet another type of organized molecular assemblies formed by the hydrophobic effect. They offer certain inherent advantages in fluorescence studies over membranes since micelles are smaller and optically transparent, have well-defined sizes, and are relatively scatter-free. Further, micelles can be of any desired charge type and can adopt different shapes and internal packing, depending on the chemical structures of the constituent monomers and the ionic strength of the medium.[29−31] The organization and dynamics of micellar environments, namely, the core, the interface, and the immediate layers of water on the interface, have been investigated using experimental[32−38] and theoretical[39] approaches. It is fairly well established now that practically all types of molecules have a surface-seeking tendency in micelles (due to very large surface area to volume ratio) and that the interfacial region is the preferred site for solubilization, even for hydrophobic molecules.[34,40−42]

In this paper, we report the observation of red edge excitation effects of NBD-PE in various types of micelles (see Figure 1) having different charges and organization [sodium dodecyl sulfate (SDS), Triton X-100, 3-[(3-cholamidopropyl)dimethylammonio]-1-propanesulfonate (CHAPS), cetyltrimethylammonium bromide (CTAB)]. NBD (7-nitrobenz-2-oxa-1,3-diazol-4-yl)-labeled lipids are widely used as fluorescent analogues of native lipids in biological and model membranes to study a variety of processes.[43,44] In NBD-PE, the NBD group is covalently attached to the headgroup of a phosphatidylethanolamine molecule. The NBD group in NBD-PE has earlier been shown to be localized in the interfacial region of the membrane[45−50] and its location in the micellar environment is most likely to be interfacial. It is thus of interest to investigate wavelength-selective fluorescence effects in micellar assemblies, especially since micelles are more dynamic structures than membranes and probably have more water in their core.[12,51]

Experimental Section

Materials. SDS, CTAB, CHAPS, and Triton X-100 were purchased from Sigma Chemical Co. (St. Louis, MO). NBD-PE, 6-[*N*-(7-nitrobenz-2-oxa-1,3-diazol-4-yl)amino]hexanoic acid (NBD-AHA), and 1,6-diphenyl-1,3,5-hexatriene (DPH) were obtained from Molecular Probes (Eugene, OR). All other chemicals used were of highest purity available. Water was purified through a Millipore (Bedford, MA) Milli-Q system and used throughout. Solvents used were of spectroscopic grade. The purity of NBD-PE was checked by thin-layer chromatography on silica gel plates in chloroform/methanol/water (65:35:5, v/v/v). It was found pure when detected by its color or fluorescence. The purity of the detergents were checked by measuring their cmc values and comparing with literature cmc. The cmc of detergents were determined fluorimetrically using a method previously developed by one of us[52] which utilizes enhancement of DPH fluorescence upon micellization.

Methods. Concentrations of detergents used were double the cmc of the respective detergent to ensure that they are in the micellar state. Thus, the concentrations of SDS, Triton X-100, CHAPS, and CTAB used were 16, 0.6, 15, and 1.76 mM, respectively. The molar ratio of fluorophore to detergent was carefully chosen to give optimum signal-to-noise ratio with minimal perturbation to the micellar organization and negligible interprobe interactions. The ratios used were 1:1000 (mol/mol) in case of CTAB and Triton X-100, and 1:10 000 (mol/mol) for SDS and CHAPS. All experiments were done at room temperature (25 °C).

Steady-state fluorescence measurements were performed with a Hitachi F-4010 spectrofluorometer using 1 cm path length quartz cuvettes. Excitation and emission slits with a nominal bandpass of 5 nm were used for all measurements. Background intensities of samples in which fluorophores were omitted were negligible in most cases and were subtracted from each sample spectrum to cancel out any contribution due to the solvent Raman peak and other scattering artifacts. Fluorescence polarization measurements were performed using a Hitachi polarization accessory. Polarization values were calculated from the equation[53]

$$P = \frac{I_{VV} - GI_{VH}}{I_{VV} + GI_{VH}} \tag{1}$$

where I_{VV} and I_{VH} are the measured fluorescence intensities (after appropriate background subtraction) with the excitation polarizer vertically oriented and emission polarizer vertically and horizontally oriented, respectively. G is the grating correction factor and is equal to I_{HV}/I_{HH}. All experiments were done with multiple sets of samples and average values of polarization are shown in the figures. The spectral shifts obtained with different sets of samples were identical in most cases. In other cases, the values were within ±1 nm of the ones reported.

Time-Resolved Fluorescence Measurements. Fluorescence lifetimes were calculated from time-resolved fluorescence intensity decays using a Photon Technology International (London, Western Ontario, Canada) LS-100 luminescence spectrophotometer in the time-correlated single-photon-counting mode. This machine uses a thyratron-gated nanosecond flash lamp filled with hydrogen as the plasma gas (17 ± 1 in. of mercury vacuum) and is run at 22−25 kHz. Lamp profiles were measured at the excitation wavelength using Ludox as the scatterer. To optimize the signal-to-noise ratio, 5000 photon counts were collected in the peak channel. All experiments were performed using slits with a nominal bandpass of 12 nm. The sample and the scatterer were alternated after every 10% acquisition to ensure compensation for shape and timing drifts occurring during the period of data collection. The data stored in a multichannel analyzer was routinely transferred to an IBM PC for analysis. Intensity decay curves so obtained were fitted as a sum of exponential terms:

$$F(t) = \sum_i \alpha_i \exp(-t/\tau_i) \tag{2}$$

where α_i is a preexponential factor representing the fractional contribution to the time-resolved decay of the component with a lifetime τ_i. The decay parameters were recovered using a nonlinear least-squares iterative fitting procedure based on the Marquardt algorithm.[54] The program also includes statistical

and plotting subroutine packages.[55] The goodness of the fit of a given set of observed data and the chosen function was evaluated by the reduced χ^2 ratio, the weighted residuals,[56] and the autocorrelation function of the weighted residuals.[57] A fit was considered acceptable when plots of the weighted residuals and the autocorrelation function showed a random deviation of about zero with a minimum χ^2 value (generally not more than 1.4). Mean (average) lifetimes $\langle\tau\rangle$ for biexponential decays of fluorescence were calculated from the decay times and preexponential factors using the following equation:

$$\langle\tau\rangle = \frac{\alpha_1\tau_1^{\,2} + \alpha_2\tau_2^{\,2}}{\alpha_1\tau_1 + \alpha_2\tau_2} \qquad (3)$$

Global Analysis of Lifetimes. The primary goal of the nonlinear least-squares (discrete) analysis of fluorescence intensity decays discussed above is to obtain an accurate and unbiased representation of a single fluorescence decay curve in terms of a set of parameters (i.e., α_i, τ_i). However, this method of analysis does not take advantage of the intrinsic relations that may exist between the individual decay curves obtained under different conditions. A condition in this context refers to temperature, pressure, solvent composition, ionic strength, pH, excitation/emission wavelength, or any other independent variable that can be experimentally manipulated. This advantage can be derived if multiple fluorescence decay curves, acquired under different conditions, are simultaneously analyzed. This is known as the global analysis in which the simultaneous analyses of multiple decay curves are carried out in terms of internally consistent sets of fitting parameters, thereby enhancing the accuracy of the recovered parameters.[58−61] Global analysis thus turns out to be very useful for the prediction of the manner in which the parameters recovered from a set of separate fluorescence decays vary as a function of an independent variable and helps distinguish between models proposed to describe a system.

In this paper, we have obtained fluorescence decays as a function of excitation and emission wavelengths. The global analysis, in this case, assumes that the lifetimes are linked among the data files (i.e., the lifetimes for any given component are the same for all decays) but that the corresponding preexponentials are free to vary. This is accomplished by using a matrix mapping of the fitting parameters in which the preexponentials are unique for each decay curve while the lifetimes are mapped out to the same value for each decay. All data files are simultaneously analyzed by the least-squares data analysis method using the Marquardt algorithm (as described above) utilizing the map to substitute parameters appropriately while minimizing the global χ^2. The software used for the global analysis was obtained from Photon Technology International (London, Western Ontario, Canada).

Results

The shifts in the maxima of fluorescence emission[62] of NBD-PE when bound to micelles of SDS, Triton X-100, CHAPS, and CTAB as a function of excitation wavelength are shown in Figure 2. The emission maximum of NBD-PE in model membranes of DOPC, in which the NBD group has been shown to be interfacial[45−50] has earlier been reported to be around 530 nm.[15,46] Figure 2 shows that upon excitation at 465 nm, the fluorescence emission maxima of NBD-PE is found to be at 532, 529, 530, and 537 nm in micelles of SDS, Triton X-100, CHAPS, and CTAB, respectively. The magnitude of these emission maxima suggest that the NBD group in NBD-PE is localized at the interfacial region of the micelles. The relatively

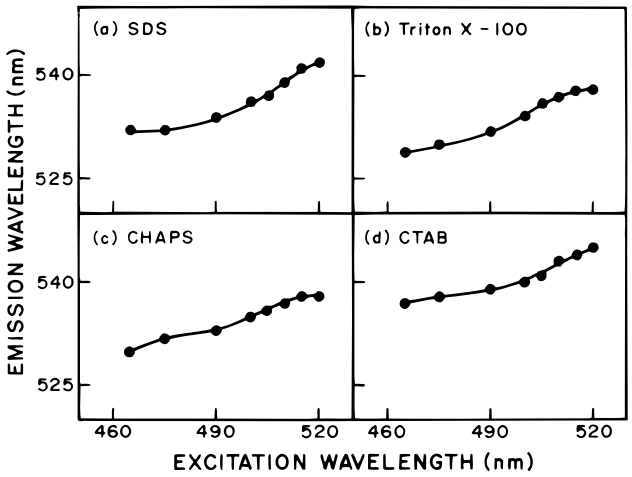

Figure 2. Effect of changing excitation wavelength on the wavelength of maximum emission for NBD-PE in micelles of (a) SDS, (b) Triton X-100, (c) CHAPS, and (d) CTAB. The ratio of NBD-PE to detergent was 1:10 000 (mol/mol) for micelles of SDS and CHAPS, and 1:1000 (mol/mol) for Triton X-100 and CTAB micelles. See Experimental Section for other details.

red-shifted emission maximum (537 nm) in case of CTAB is possibly due to the electrostatic interaction between NBD-PE which is negatively charged at physiological pH[46] and the positively charged CTAB molecules. As the excitation wavelength is changed from 465 to 520 nm, the emission maxima of micelle-bound NBD-PE are shifted from 532 to 542 nm (in case of SDS micelles), 529 to 538 nm (Triton X-100), 530 to 538 nm (CHAPS), and 537 to 545 nm (CTAB), which correspond to REES of 8−10 nm in each of these cases. Such dependence of the emission spectra on the excitation wavelength is characteristic of the red edge effect. Observation of this effect in micelles implies that the NBD group of NBD-PE, when incorporated in these micelles, is in an environment where its mobility is considerably reduced. Since the NBD group is thought to be localized in the micellar interfacial region (see above), such a result would directly imply that this region of the micelle offers considerable restriction to the reorientational motion of the solvent dipoles around the excited-state fluorophore. In a control experiment (not shown), we monitored the effect of changing excitation wavelength on the emission maximum of NBD-AHA (NBD-labeled fatty acid) incorporated into detergent solutions in premicellar concentrations. There was no significant REES in these cases indicating that the micellar organization around the fluorophore is responsible for the above red edge effects. NBD-PE was not used in these experiments because it tends to form mixed micelles with these detergents even at premicellar concentrations since its own critical bilayer concentration is much lower.[63]

In addition to the dependence of fluorescence emission maxima on the excitation wavelength, fluorescence polarization is also known to depend on the excitation wavelength in viscous solutions or in otherwise motionally restricted media (refs 15−17 and 20 and references therein). Due to strong dipolar interactions with the surrounding solvent molecules, there is a decreased rotational rate of the fluorophore in the relaxed state. On red edge excitation, a selective excitation of this subclass of fluorophore occurs. Because of strong interaction with the polar solvent molecules in the excited state, one may expect these "solvent relaxed" fluorophores to rotate more slowly, thereby increasing the polarization.

The excitation polarization spectra (i.e., a plot of steady-state polarization vs excitation wavelength) of NBD-PE in micelles of SDS, Triton X-100, CHAPS, and CTAB are shown in Figure

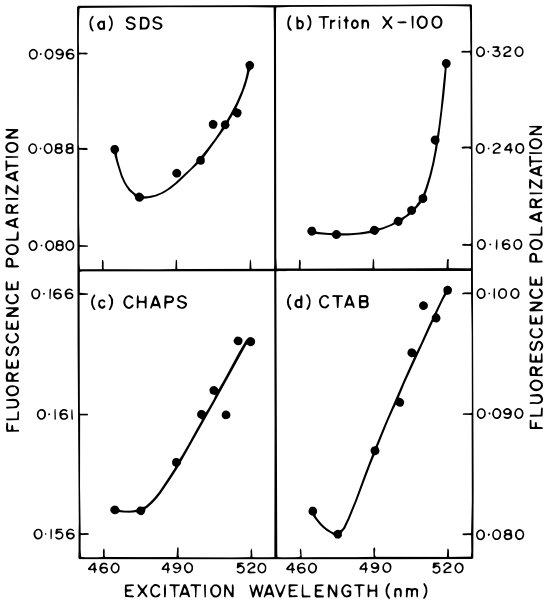

Figure 3. Fluorescence polarization of NBD-PE as a function of excitation wavelength in micelles of (a) SDS, (b) Triton X-100, (c) CHAPS, and (d) CTAB. Polarization values were recorded at 535 nm for micelles of SDS and Triton X-100, and at 540 nm for CHAPS and CTAB micelles. All other conditions are as in Figure 2. See Experimental Section for other details.

3. The polarization of NBD-PE in these micelles undergoes considerable change upon altering the excitation wavelength, with a sharp increase occurring toward the red edge of the absorption band. Such an increase in polarization upon red edge excitation for peptides and proteins containing tryptophans as well as other aromatic fluorophore, especially in media of reduced mobility such as propylene glycol at low temperature, has been previously reported. This reinforces our earlier conclusion that the NBD group in NBD-PE is in a motionally restricted region when bound to micelles. It is interesting to note here that the polarization values are in general higher in electrically neutral micelles (such as Triton X-100 and CHAPS) compared to those in charged micelles (such as SDS and CTAB). This could reflect the differences in packing arrangements of the detergent monomers in the two types of micelles as experienced by the micelle-bound NBD group, the packing being tighter in neutral micelles owing to smaller water content in the interfacial region (see Discussion).

The origin of the red edge effect lies in differential extents of solvent reorientation around the excited-state fluorophore, with each excitation wavelength selectively exciting a different average population of fluorophores.[20,21] Since fluorescence lifetime serves as a sensitive indicator for the local environment in which a given fluorophore is placed and is known to be sensitive to excited-state interactions, differential extents of solvent relaxation around a given fluorophore could be expected to give rise to differences in its lifetime. Table 1 shows the lifetimes of NBD-PE in micelles of SDS, Triton X-100, CHAPS, and CTAB as a function of excitation wavelength, keeping the emission wavelength constant. All fluorescence decays for micelle-bound NBD-PE could be fitted well with biexponential function. As can be seen from the table, when micelle-bound NBD-PE is excited at its mean excitation wavelength, i.e., 465 nm, the decay fits a biexponential function, with a relatively short lifetime component (1.13−2.79 ns) and a longer lifetime component (3.05−7.29 ns), with mean lifetimes (see Figure 6) of 2.69 ns (in case of SDS micelles), 4.44 ns (Triton X-100), 5.97 ns (CHAPS), and 2.88 ns (for CTAB micelles). We attribute this difference in mean fluorescence lifetime of NBD-PE in various types of micelles to a combination of factors such as the exact site of localization of the fluorophore which will be somewhat different in individual cases due to differences in shape and size of different types of micelles as well as the water content in the region of probe localization (see later). A typical decay profile with its biexponential fitting and the various

TABLE 1: Lifetimes of NBD-PE as a Function of Excitation Wavelength

excitation wavelength (nm)	α_1	τ_1 (ns)	α_2	τ_2 (ns)
		(a) SDS[a]		
465	0.38 ± 0.02 (0.49)[c]	1.39 ± 0.12 (0.37)	0.62 ± 0.03 (0.51)	3.05 ± 0.04 (2.83)
480	0.41 ± 0.00 (0.66)	0.58 ± 0.01 (0.37)	0.59 ± 0.00 (0.34)	2.87 ± 0.00 (2.83)
490	0.51 ± 0.10 (0.62)	0.67 ± 0.13 (0.37)	0.49 ± 0.01 (0.38)	2.93 ± 0.02 (2.83)
500	0.68 ± 0.00 (0.53)	0.30 ± 0.00 (0.37)	0.32 ± 0.00 (0.47)	2.93 ± 0.00 (2.83)
505	0.83 ± 0.14 (0.78)	0.29 ± 0.05 (0.37)	0.17 ± 0.00 (0.22)	2.95 ± 0.02 (2.83)
510	0.95 ± 0.00 (0.95)	0.35 ± 0.00 (0.37)	0.05 ± 0.00 (0.05)	3.20 ± 0.00 (2.83)
		(b) Triton X-100[a]		
465	0.48 ± 0.02 (0.65)	1.26 ± 0.07 (0.38)	0.52 ± 0.01 (0.35)	5.16 ± 0.03 (4.73)
480	0.51 ± 0.01 (0.67)	1.93 ± 0.09 (0.38)	0.49 ± 0.00 (0.33)	5.49 ± 0.04 (4.73)
490	0.63 ± 0.00 (0.76)	0.93 ± 0.00 (0.38)	0.37 ± 0.00 (0.24)	5.19 ± 0.00 (4.73)
500	0.92 ± 0.00 (0.89)	0.41 ± 0.00 (0.38)	0.08 ± 0.00 (0.11)	5.36 ± 0.01 (4.73)
510	0.96 ± 0.00 (0.96)	0.36 ± 0.00 (0.38)	0.04 ± 0.00 (0.04)	4.61 ± 0.00 (4.73)
		(c) CHAPS[a]		
465	0.52 ± 0.00 (0.75)	2.79 ± 0.00 (0.26)	0.48 ± 0.00 (0.25)	7.29 ± 0.00 (5.79)
480	0.49 ± 0.01 (0.74)	2.64 ± 0.05 (0.26)	0.51 ± 0.00 (0.26)	7.09 ± 0.03 (5.79)
490	0.62 ± 0.01[d]	3.38 ± 0.10	0.38 ± 0.02	7.80 ± 0.09
500	0.68 ± 0.04[d]	1.28 ± 0.05	0.32 ± 0.00	6.74 ± 0.04
505	0.80 ± 0.00 (0.94)	1.17 ± 0.05 (0.26)	0.20 ± 0.03 (0.06)	6.49 ± 0.04 (5.79)
510	0.97 ± 0.00 (0.97)	0.28 ± 0.00 (0.26)	0.03 ± 0.00 (0.03)	6.13 ± 0.01 (5.79)
		(d) CTAB[b]		
465	0.60 ± 0.02 (0.60)	1.13 ± 0.07 (0.99)	0.40 ± 0.01 (0.40)	3.68 ± 0.03 (3.59)
480	0.62 ± 0.02 (0.56)	1.64 ± 0.08 (0.99)	0.38 ± 0.02 (0.44)	3.97 ± 0.06 (3.59)
490	0.59 ± 0.01 (0.57)	1.30 ± 0.02 (0.99)	0.41 ± 0.00 (0.43)	3.79 ± 0.02 (3.59)
500	0.66 ± 0.04 (0.57)	1.16 ± 0.08 (0.99)	0.34 ± 0.01 (0.43)	3.98 ± 0.05 (3.59)
505	0.80 ± 0.01 (0.78)	1.21 ± 0.04 (0.99)	0.20 ± 0.01 (0.22)	3.91 ± 0.06 (3.59)
510	0.90 ± 0.05 (0.89)	0.85 ± 0.05 (0.99)	0.10 ± 0.00 (0.11)	4.22 ± 0.05 (3.59)

[a] Emission wavelength 531 nm. [b] Emission wavelength 540 nm. [c] Number in parentheses are the results of global analysis. [d] Global analysis of these data were not performed since the position of the peak channel was different for the decay profiles relative to others in this set.

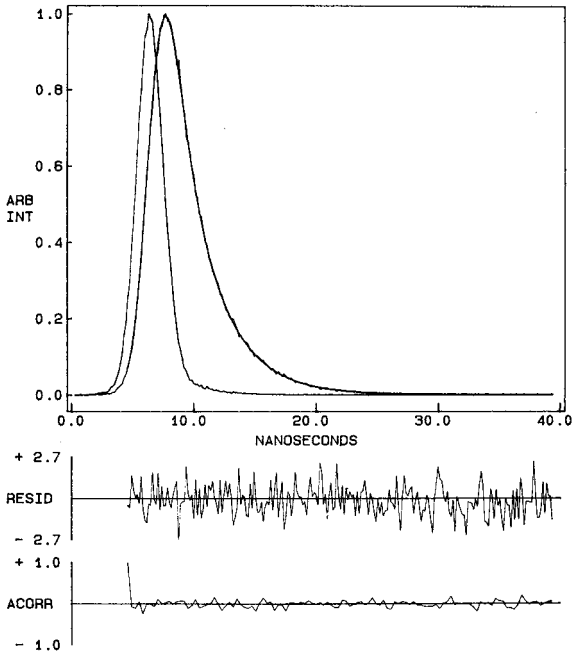

Figure 4. Time-resolved fluorescence intensity decay of NBD-PE in SDS micelles when excited at 465 nm. Emission was monitored at 531 nm. The sharp peak on the left is the lamp profile. The relatively broad peak on the right is the decay profile, fitted to a biexponential function. The two lower plots show the weighted residuals and the autocorrelation function of the weighted residuals. The ratio of NBD-PE to SDS was 1:10 000 (mol/mol). All other conditions are as in Figure 2. See Experimental Section for other details.

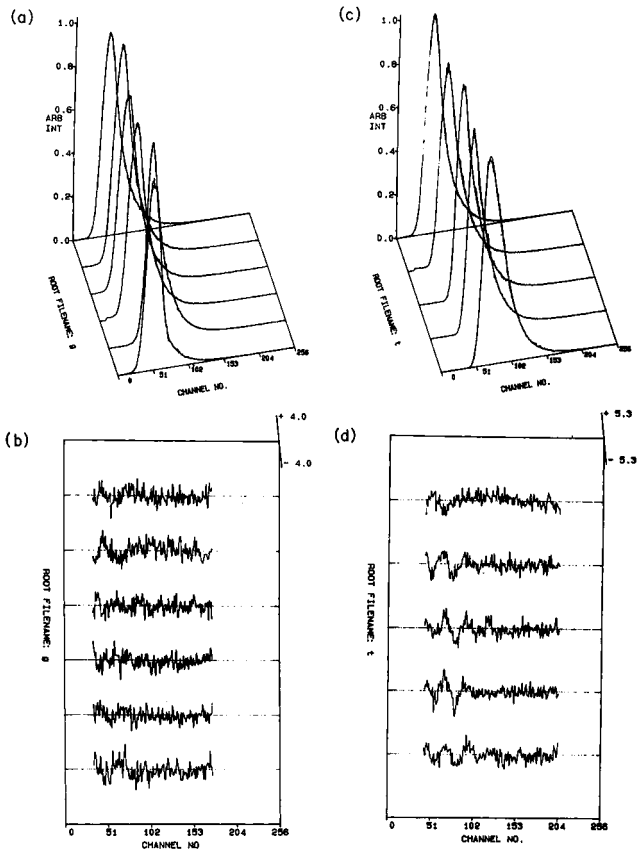

Figure 5. Global fittings and the corresponding weighted residuals of the set of decay profiles of NBD-PE in SDS micelles obtained as a function of excitation wavelength (a and b), and emission wavelength (c and d). All other conditions are as in Figure 2. See Experimental Section for other details.

statistical parameter used to check the goodness of the fit is shown in Figure 4.

The fluorescence lifetime of NBD group in NBD-AHA has previously been reported to be about 7−10 ns in various aprotic solvents.[64] The lifetime of the NBD moiety in case of dilauroyl and dimyristoyl NBD-PE incorporated in vesicles of egg phosphatidylcholine has previously been reported to be 6−8 ns.[65] The lifetime of NBD-PE incorporated into DOPC vesicles has been reported to be ∼7.4 ns.[15] In water, however, NBD lifetime reduces to ∼1.5 ns, which has been attributed to hydrogen-bonding interactions between the fluorophore and the solvent[64] which is accompanied by an increase in the rate of nonradiative decay.[44] Our results show that the lifetimes of NBD-PE when incorporated into micelles, in general, are smaller than the lifetime obtained for membrane-bound NBD-PE. This could be due to greater water content in the micellar interface compared to the membrane interface because of packing differences in these two types of organized assemblies. Further, the NBD lifetimes in micelles carrying a net electrical charge such as SDS and CTAB are considerably reduced than the lifetimes obtained with neutral micelles such as Triton X-100 and CHAPS, indicating more water content in the charged micelles.

When the excitation wavelength was gradually shifted toward the red edge of the absorption band (keeping the emission wavelength constant), it was found that although the long-lifetime component did not change significantly, there was a change in the short-lifetime component (see Table 1). Interestingly, the preexponential factor for the short-lifetime component increased steadily with shift in the excitation wavelength toward the red edge, with a concomitant reduction of the preexponential factor for the relatively long-lifetime component.

To confirm the above interpretation, the same set of fluorescence decays was subjected to global analysis. The decays were all assumed to be biexponential (on the basis of the results from discrete analysis), with lifetime components that were assumed to be linked among the data files and whose relative contributions (preexponential factors) were allowed to vary. The results of the global analysis are shown in parentheses in Table 1 and are found to be consistent with the above interpretation. The fittings of the set of decay profiles analyzed by the global method are presented as a pseudo-three-dimensional plot of intensity vs time vs increasing file number in Figure 5a. The weighted residuals corresponding to each of these fittings are also shown (Figure 5b). The normalized global χ^2 values obtained were 1.26, 1.25, 1.27, and 1.27 for the data sets in case of SDS, Triton X-100, CHAPS, and CTAB micelles, respectively.

The mean fluorescence lifetimes of micelle-bound NBD-PE were calculated using eq 3 and are plotted as a function of excitation wavelength in Figure 6 for both discrete and global analysis. As shown in this figure, there is a steady decrease in the mean lifetimes of NBD-PE with increasing excitation wavelength from 465 to 510 nm, irrespective of the method of analysis (discrete or global). Such a marked shortening of mean fluorescence lifetime at the red edge of the absorption band is indicative of slow solvent reorientation around the excited state fluorophore.[15,17,20]

Table 2 shows the lifetimes of micelle-bound NBD-PE as a function of emission wavelength, keeping the excitation wavelength constant at 465 nm. All decays corresponding to different emission wavelengths could be fitted to biexponential functions. Global analysis of this set of fluorescence decays was performed as mentioned above (assuming all decays to be biexponential with fixed lifetime components and varying preexponential

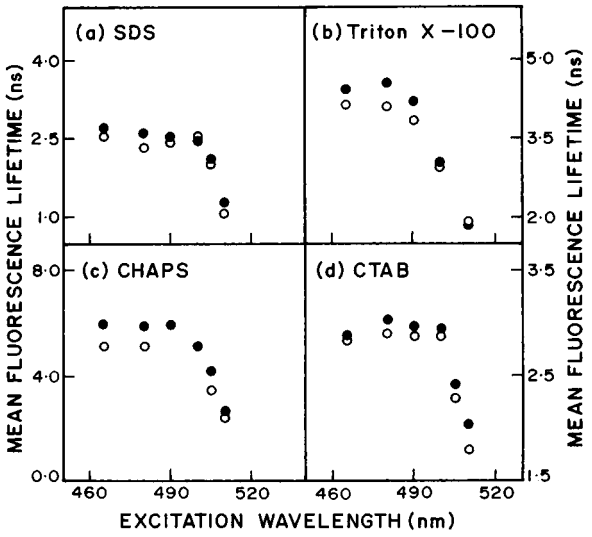

Figure 6. Mean fluorescence lifetime of NBD-PE as a function of excitation wavelength in micelles of (a) SDS, (b) Triton X-100, (c) CHAPS, and (d) CTAB obtained by (●) discrete analysis, and (○) global analysis. Emission wavelength was kept constant at 531 nm for micelles of SDS, Triton X-100, and CHAPS, while for CTAB micelles it was 540 nm. Mean lifetimes were calculated from Table 1 using eq 3. All other conditions are as in Figure 2. See Experimental Section for other details.

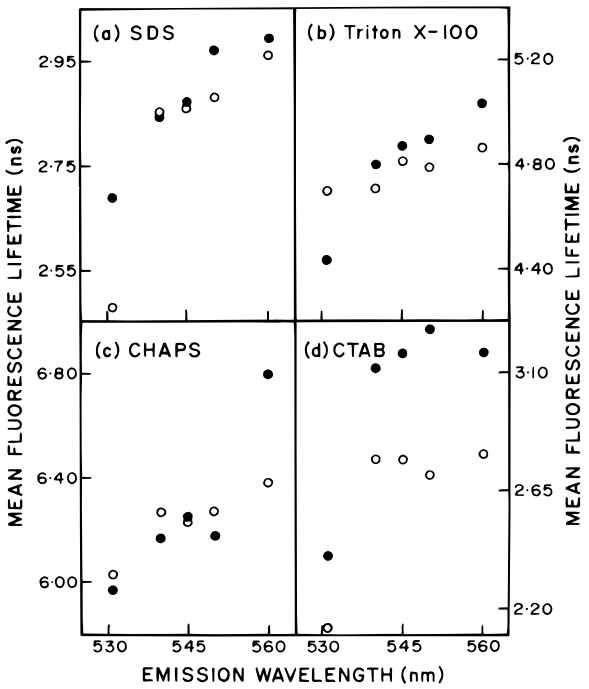

Figure 7. Mean fluorescence lifetime of NBD-PE as a function of emission wavelength in micelles of (a) SDS, (b) Triton X-100, (c) CHAPS, and (d) CTAB obtained by (●) discrete analysis, and (○) global analysis. Excitation wavelength used was 465 nm. Mean lifetimes were calculated from Table 2 using eq 3. All other conditions are as in Figure 2. See Experimental Section for other details.

factors) and the results of global analysis are shown in parentheses in Table 2. The fittings of the set of decay profiles analyzed by the global method are presented as a pseudo-three-dimensional plot of intensity vs time vs increasing file number in Figure 5c. The weighted residuals corresponding to each of these fittings are shown in Figure 5d. The normalized global χ^2 values obtained were 1.82, 1.09, 1.16, and 1.39 for the data sets in case of SDS, Triton X-100, CHAPS, and CTAB micelles, respectively. The mean lifetimes, calculated using eq 3, are plotted as a function of emission wavelength in Figure 7 for both discrete and global analysis. As shown in this figure, there is a considerable increase in mean lifetime with increasing emission wavelength from 531 to 560 nm which is independent of the method of analysis (discrete or global). Similar observations have previously been reported for fluorophores in environments of restricted mobility.[15,17,20] Such increasing lifetimes across the emission spectrum may be interpreted in terms of solvent reorientation around the excited-state fluorophore as follows. Observation at shorter wavelengths of emission spectra selects for predominantly unrelaxed fluorophores. Their lifetimes are shorter because this population is decaying both at the rate of fluorescence emission at the given excitation

TABLE 2: Lifetimes of NBD-PE as a Function of Emission Wavelength[a]

emission wavelength (nm)	α_1	τ_1 (ns)	α_2	τ_2 (ns)
		(a) SDS		
531	0.38 ± 0.02 (0.63)[b]	1.39 ± 0.12 (0.56)	0.62 ± 0.03 (0.37)	3.05 ± 0.04 (3.08)
540	0.60 ± 0.00 (0.35)	0.25 ± 0.00 (0.56)	0.40 ± 0.00 (0.65)	3.15 ± 0.00 (3.08)
545	0.58 ± 0.00 (0.28)	0.28 ± 0.00 (0.56)	0.42 ± 0.00 (0.66)	3.18 ± 0.00 (3.08)
550	0.97 ± 0.02 (0.32)	2.82 ± 0.06 (0.56)	0.03 ± 0.03 (0.68)	5.53 ± 1.07 (3.08)
560	0.76 ± 0.19 (0.22)	3.19 ± 0.14 (0.56)	0.24 ± 0.17 (0.78)	1.93 ± 0.73 (3.08)
		(b) Triton X-100		
531	0.48 ± 0.02 (0.41)	1.26 ± 0.07 (3.10)	0.52 ± 0.01 (0.59)	5.16 ± 0.03 (5.34)
540	0.53 ± 0.00 (0.40)	3.22 ± 0.03 (3.10)	0.47 ± 0.00 (0.60)	5.79 ± 0.02 (5.34)
545	0.68 ± 0.12 (0.35)	3.85 ± 0.27 (3.10)	0.32 ± 0.13 (0.65)	6.22 ± 0.45 (5.34)
550	0.52 ± 0.09 (0.36)	3.42 ± 0.30 (3.10)	0.48 ± 0.10 (0.64)	5.83 ± 0.26 (5.34)
560	0.93 ± 0.02 (0.32)	4.53 ± 0.06 (3.10)	0.07 ± 0.02 (0.68)	8.54 ± 0.71 (5.34)
		(c) CHAPS		
531	0.52 ± 0.00 (0.60)	2.79 ± 0.00 (3.67)	0.48 ± 0.00 (0.40)	7.29 ± 0.00 (7.72)
540	0.57 ± 0.04 (0.54)	3.76 ± 0.23 (3.67)	0.43 ± 0.05 (0.46)	7.72 ± 0.25 (7.72)
545	0.62 ± 0.02 (0.55)	3.94 ± 0.12 (3.67)	0.38 ± 0.02 (0.45)	8.09 ± 0.12 (7.72)
550	0.54 ± 0.01 (0.54)	3.44 ± 0.07 (3.67)	0.46 ± 0.01 (0.46)	7.63 ± 0.04 (7.72)
560	0.47 ± 0.02 (0.51)	3.75 ± 0.15 (3.67)	0.53 ± 0.02 (0.49)	7.54 ± 0.08 (7.72)
		(d) CTAB		
531	0.80 ± 0.01 (0.80)	1.08 ± 0.02 (0.78)	0.20 ± 0.00 (0.20)	3.87 ± 0.03 (3.38)
540	0.60 ± 0.02 (0.57)	1.13 ± 0.07 (0.78)	0.40 ± 0.01 (0.43)	3.68 ± 0.03 (3.38)
545	0.59 ± 0.01 (0.57)	1.33 ± 0.04 (0.78)	0.41 ± 0.01 (0.43)	3.73 ± 0.03 (3.38)
550	0.68 ± 0.02 (0.60)	1.83 ± 0.09 (0.78)	0.32 ± 0.03 (0.40)	4.08 ± 0.08 (3.38)
560	0.59 ± 0.01 (0.56)	1.37 ± 0.07 (0.78)	0.41 ± 0.02 (0.44)	3.74 ± 0.05 (3.38)

[a] Excitation wavelength 465 nm. [b] Number in parentheses are the results of global analysis.

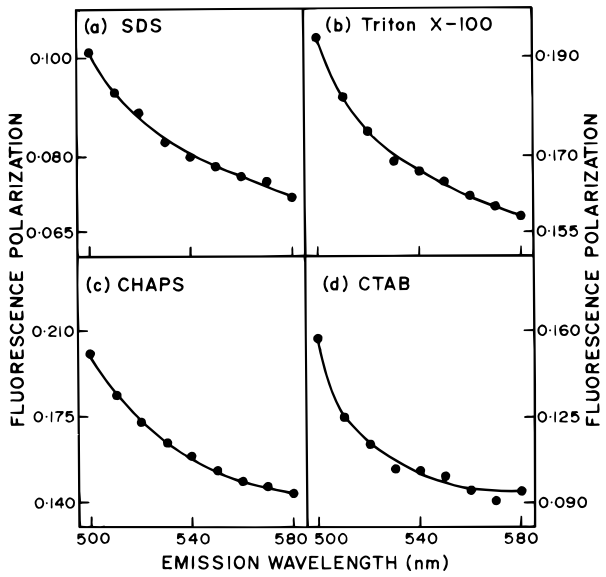

Figure 8. Fluorescence polarization of NBD-PE as a function of emission wavelength in micelles of (a) SDS, (b) Triton X-100, (c) CHAPS, and (d) CTAB. The excitation wavelength was 465 nm in all cases. All other conditions are as in Figure 2. See Experimental Section for other details.

wavelength and by decay to longer (unobserved) wavelengths. In contrast, observation at the long-wavelength (red) edge of the emission selects for the more relaxed fluorophores, which have spent enough time in the excited state to allow increasingly larger extents of solvent relaxations.

These longer-lived fluorophores, which are also those which emit at higher wavelengths, should, in principle, have more time to rotate in the excited state, giving rise to lower polarization. Figure 8 shows the variation in the steady-state polarization of NBD-PE in various micelles as a function of wavelength across its emission spectrum. As seen in the figure, there is a considerable decrease in polarization with increasing emission wavelength in all cases. The lowest polarization is observed toward longer wavelengths (red edge) where emission from the relaxed fluorophores predominates. Similar observations have previously been reported for other fluorophores in environments of restricted mobility.[15−17,20,66] This gives further support to our interpretation of the wavelength-selective fluorescence effects for NBD-PE incorporated into micelles.

Discussion

Wavelength-selective fluorescence has been previously applied for monitoring protein dynamics and conformation in solution[19,67−71] as well as in more complex systems such as the intact eye lens.[72,73] We have previously applied this approach for studying organization and dynamics of membrane-bound probes and peptides.[15−17] Application of the wavelength-selective fluorescence approach to micellar organization and dynamics has been the focus of this report. We show here that NBD-PE, when incorporated into micelles of different charges and organization (SDS, Triton X-100, CHAPS, and CTAB), exhibits wavelength-selective fluorescence effects. This implies that the NBD group of NBD-PE, when bound to micelles, is in a motionally restricted environment. Furthermore, since the NBD group is most likely to be localized in the micellar interfacial region, our results show that this region of the micelle offers considerable restriction to the reorientational motion of the solvent dipoles around the excited-state fluorophore. To the best of our knowledge, this is the first report describing the application of this approach to micellar systems. The detergents chosen for this study represent various classes of detergents used in isolation and solubilization of membrane proteins[74−79] and also as membrane mimetics for characterizing membrane proteins and peptides.[5−8]

The choice of a suitable probe is of considerable importance in wavelength-selective fluorescence studies of organized molecular assemblies such as membranes or micelles.[15] The probe chosen for this work (NBD-PE) is appropriate, because the location of the NBD group in NBD-PE is expected to be interfacial, a region in the micellar organization, which acts as a preferred site for solubilization[34,40−42] and is characterized by unique motional and dielectric characteristics.[37,38,80] This region has been implicated to have a major role in reactions catalyzed by micelles.[81] The lower polarity of this region can provide stability to the transition state or destabilize the substrate, which can accelerate the product formation. The restricted environment, on the other hand, can be significant in increasing the effective concentration of the substrate causing an increase in reaction rate required for catalysis.

The NBD group possesses some of the most desirable properties for serving as an excellent probe for both spectroscopic as well as microscopic applications.[82] It is very weakly fluorescent in water. Upon transfer to hydrophobic media, it fluoresces brightly in the visible range and shows a large degree of environmental sensitivity.[18,46,64,83,84] This large degree of environmental sensitivity of NBD fluorescence can prove to be very useful in probing different types of micellar organizations formed by various detergents. For example, the lifetimes of NBD-PE in charged micelles are considerably shorter than lifetimes observed in neutral micelles. Since NBD lifetimes are known to be shortened in the presence of water,[44,64] this enables us to comment on the extent of water penetration in various micelles. In general, charged detergents form micelles with greater interheadgroup spacing due to electrostatic repulsions between the headgroups, which can result in more water in the space between the headgroups. The interheadgroup spacing in an uncharged (Triton X-100) or zwitterionic detergent (CHAPS) is relatively small leading to less amount of water trapped between the headgroups. The extent of hydration modulates the dielectric properties of the interfacial region.[85] The shorter lifetimes observed in our studies in case of the charged micelles are indicative of this effect.

The ability of a micelle-bound fluorophore to exhibit red edge effects will depend on a number of factors such as its polarity, as well as the effective polarity of its immediate environment, and its fluorescence characteristics (e.g., lifetime). Since all these properties of a probe in a micelle are a function of its location in the micelle, the extent of REES could very well be dependent on its location in the micelle. Wavelength-selective fluorescence promises to be a powerful approach for monitoring micellar organization and dynamics including conformation and dynamics of peptides and proteins incorporated into such assemblies.

Acknowledgment. We thank Y.S.S.V. Prasad and G.G. Kingi for technical help. This work was supported by the Council of Scientific and Industrial Research, Government of India. S.S.R. thanks the Council of Scientific & Industrial Research for the award of a Junior Research Fellowship. S.M. was awarded a Senior Research Fellowship by the University Grants Commission. The Photon Technology International LS-100 luminescence spectrophotometer used in this study was purchased from a grant awarded by the Department of Science and Technology, Government of India.

References and Notes

(1) Tanford, C. *Science* **1978**, *200*, 1012.
(2) Israelachvili, J. N.; Marcelja, S.; Horn, R. G. *Q. Rev. Biophys.* **1980**, *13*, 121.
(3) Tanford, C. *The Hydrophobic Effect: Formation of Micelles and Biological Membranes*; Wiley-Interscience: New York, 1980.
(4) Tanford, C. *Biochem. Soc. Trans.* **1987**, *15*, 1S.
(5) Franklin, J. C.; Ellena, J. F.; Jayasinghe, S.; Kelsh, L. P.; Cafiso, D. S. *Biochemistry* **1994**, *33*, 4036.
(6) Improta, S.; Pastore, A.; Mammi, S.; Peggion, E. *Biopolymers* **1994**, *34*, 773.
(7) Lenz, V. J.; Federwisch, M.;. Gattner, H.-G.; Brandenburg, D.; Hocker, H.; Hassiepen, U.; Wollner, A. *Biochemistry* **1995**, *34*, 6130.
(8) Mattice, G. L.; Koeppe, R. E.; Providence, L. L.; Andersen, O. S. *Biochemistry* **1995**, *34*, 6827.
(9) Desai, S.; Hadlock, T.; Messam,C.; Chafetz, R.; Strichartz, G. *J. Pharmacol. Exp. Ther.* **1994**, *271*, 220.
(10) Laval, J.-M.; Chopineau, J.; Thomas, D. *Trends Biotechnol.* **1995**, *13*, 474.
(11) Lehninger, A. L., Nelson, D. L.; Cox, M. M. *Principles of Biochemistry*; Worth Publishers: New York, 1993; pp 480−481.
(12) Menger, F. M. *Acc. Chem. Res.* **1979**, *12*, 111.
(13) Lindman, B.; Wennerstrom, H. In *Solution Behavior of Surfactants: Theoretical and Applied Aspects*; Mittal, K. L., Fendler, E. J., Eds.; Plenum Press: New York, 1982; Vol. 1, pp 3−25.
(14) Chattopadhyay, A. *Biophys. J.* **1991**, *59*, 191a.
(15) Chattopadhyay, A.; Mukherjee, S. *Biochemistry* **1993**, *32*, 3804.
(16) Chattopadhyay, A; Rukmini, R. *FEBS Lett.* **1993**, *35*, 341.
(17) Mukherjee, S.; Chattopadhyay, A. *Biochemistry* **1994**, *33*, 5089.
(18) Mukherjee, S.; Chattopadhyay, A.; Samanta, A.; Soujanya, T. *J. Phys. Chem.* **1994**, *98*, 2809.
(19) Guha, S.; Rawat, S. S.; Chattopadhyay, A.; Bhattacharyya, B. *Biochemistry* **1996**, *35*, 13426.
(20) Mukherjee, S.; Chattopadhyay, A. *J. Fluorescence* **1995**, *5*, 237.
(21) Demchenko, A. P. *Trends Biochem. Sci.* **1988**, *13*, 374.
(22) Ho, C.; Stubbs, C. D. *Biophys. J.* **1992**, *63*, 897.
(23) Fischer, W. B.; Sonar, S.; Marti, T.; Khorana, H. G.; Rothschild, K. J. *Biochemistry* **1994**, *33*, 12757.
(24) Kandori, H.; Yamazaki, Y.; Sasaki, J.; Needleman, R.; Lanyi, J. K.; Maeda, A. *J. Am. Chem. Soc.* **1995**, *117*, 2118.
(25) Sankararamakrishnan, R.; Sansom, M. S. P. *FEBS Lett.* **1995**, *377*, 377.
(26) Ghosh, A. K.; Rukmini, R.; Chattopadhyay, A., unpublished observations.
(27) Becker, M. D., Greathouse, D. V.; Koeppe, R. E.; Andersen, O. S. *Biochemistry* **1991**, *30*, 8830.
(28) Blondelle, S. E.; Houghten, R. A. *Biochemistry* **1991**, *30*, 4671.
(29) Missel, P. J.; Mazer, N. A.; Carey, M. C.; Benedek, G. B. In *Solution Behavior of Surfactants: Theoretical and Applied Aspects*; Mittal, K. L., Fendler, E. J., Eds.; Plenum Press: New York, 1982; pp 373−388.
(30) Ikeda, S. In *Surfactants in Solution*; Mittal, K. L., Fendler, E. J., Eds.; Plenum Press: New York, 1984; Vol. 2, pp 825−840.
(31) Porte, G.; Appell, J. In *Surfactants in Solution*; Mittal, K. L., Fendler, E. J., Eds.; Plenum Press: New York, 1984; Vol. 2, pp 805−823.
(32) Shinitzky, M.; Dianoux, A.-C.; Gitler, C.; Weber, G. *Biochemistry* **1971**, *10*, 2106.
(33) Kalyanasundaram, K.; Thomas, J. K. *J. Phys. Chem.* **1977**, *81*, 2176.
(34) Mukerjee, P.; Cardinal, J. R. *J. Phys. Chem.* **1978**, *82*, 1620.
(35) Leung, R.; Shah, D. O. *J. Colloid Interface Sci.* **1986**, *113*, 484.
(36) Nery, H.; Soderman, O.; Canet, D.; Walderhaug, H.; Lindman, B. *J. Phys. Chem.* **1986**, *90*, 5802.
(37) Maiti, N. C.; Mazumdar, S.; Periasamy, N. *J. Phys. Chem.* **1995**, *99*, 10708.
(38) Saroja, G.; Samanta, A. *Chem. Phys. Lett.* **1995**, *246*, 506.
(39) Gruen, D. W. R. *J. Phys. Chem.* **1985**, *89*, 153.
(40) Ganesh, K. N.; Mitra, P.; Balasubramanian, D. *J. Phys. Chem.* **1982**, *86*, 4291.
(41) Shobha, J.; Balasubramanian, D. *J. Phys. Chem.* **1986**, *90*, 2800.
(42) Shobha, J., Srinivas, V.; Balasubramanian, D. *J. Phys. Chem.* **1989**, *93*, 17.
(43) Chattopadhyay, A. *Chem. Phys. Lipids* **1990**, *53*, 1.
(44) Mazeres, S.; Schram, V.; Tocanne, J.-F.; Lopez, A. *Biophys. J.* **1996**, *71*, 327.
(45) Chattopadhyay, A.; London, E. *Biochemistry* **1987**, *26*, 39.
(46) Chattopadhyay, A.; London, E. *Biochim. Biophys. Acta.* **1988**, *938*, 24.
(47) Pagano, R. E.; Martin, O. C. *Biochemistry* **1988**, *27*, 4439.
(48) Mitra, B.; Hammes, G. G. *Biochemistry* **1990**, *29*, 9879.
(49) Wolf, D. E.; Winiski, A. P.; Ting, A. E.; Bocian, K. M.; Pagano, R. E. *Biochemistry* **1992**, *31*, 2865.
(50) Abrams, F. S.; London, E. *Biochemistry* **1993**, *32*, 10826.
(51) Ganesh, K. N.; Mitra, P.; Balasubramanian, D. In *Surfactants in Solution*; Mittal, K. L., Lindman, B., Eds.; Plenum Press: New York, 1984; Vol. 1, pp 599−611.
(52) Chattopadhyay, A.; London, E. *Anal. Biochem.* **1984**, *139*, 408.
(53) Chen, R. F.; Bowman, R. L. *Science* **1965**, *147*, 729.
(54) Bevington, P. R. *Data reduction and error analysis for the physical sciences*; McGraw-Hill: New York, 1969.
(55) O'Connor, D. V.; Phillips, D. *Time-Correlated Single Photon Counting*; Academic Press: London, 1984; pp 180−189.
(56) Lampert, R. A.; Chewter, L. A.; Phillips, D.; O'Connor, D. V.; Roberts, A. J.; Meech, S. R. *Anal. Chem.* **1983**, *55*, 68.
(57) Grinvald, A.; Steinberg, I. Z. *Anal. Biochem.* **1974**, *59*, 583.
(58) Knutson, J. R.; Beechem, J. M.; Brand, L. *Chem. Phys. Lett.* **1983**, *102*, 501.
(59) Beechem, J. M. *Chem. Phys. Lipids* **1989**, *50*, 237.
(60) Beechem, J. M. *Meth. Enzymol.* **1992**, *210*, 37.
(61) Beechem, J. M.; Gratton, E.; Ameloot, M.; Knutson, J. R.; Brand, L. In *Topics in Fluorescence Spectroscopy: Principles*; Lakowicz, J. R., Ed.; Plenum Press: New York, 1991; Vol. 2, pp 241−305.
(62) We have used the term maximum of fluorescence emission in a somewhat wider sense here. In every case, we have monitored the wavelength corresponding to maximum fluorescence intensity, as well as the center of mass of the fluorescence emission. In most cases, both these methods yielded the same wavelength. In cases where minor discrepancies were found, the center of mass of emission has been reported as the fluorescence maximum.
(63) Smith, R.; Tanford, C. *J. Mol. Biol.* **1972**, *67*, 75.
(64) Lin, S.; Struve, W. S. *Photochem. Photobiol.* **1991**, *54*, 361.
(65) Arvinte, T.; Cudd., A.; Hildenbrand, K. *Biochim. Biophys. Acta*. **1986**, *860*, 215.
(66) Sommer, A.; Paltauf, F.; Hermetter, A. *Biochemistry* **1990**, *29*, 11134.
(67) Demchenko, A. P. *Biophys. Chem.* **1982**, *15*, 101.
(68) Demchenko, A. P. *Eur. Biophys. J.* **1988**, *16*, 121.
(69) Demchenko, A. P.; Ladokhin, A. S. *Eur. Biophys. J.* **1988**, *15*, 369.
(70) Wasylewski, Z.; Koloczek, H.; Wasniowska, A.; Slizowska, K. *Eur. J. Biochem.* **1992**, *206*, 235.
(71) Demchenko, A. P.; Gryczynski, I.; Gryczynski, Z.; Wiczk, W.; Malak, H.; Fishman, M. *Biophys. Chem.* **1993**, *48*, 39.
(72) Rao, S. C.; Rao, Ch. M. *FEBS Lett.* **1994**, *337*, 269.
(73) Rao, Ch. M.; Rao, S. C.; Rao, P. B. *Photochem. Photobiol.* **1989**, *50*, 399.
(74) Helenius, A.; Simons, K. *Biochim. Biophys. Acta* **1975**, *415*, 29.
(75) Helenius, A.; McCaslin, D. R.; Fries, E.; Tanford, C. *Meth. Enzymol.* **1979**, *56*, 734.
(76) Hjelmeland, L. M. *Proc. Natl. Acad. Sci. U.S.A.* **1980**, *77*, 6368.
(77) Lichtenberg, D.; Robson, R. J.; Dennis, E. A. *Biochim. Biophys. Acta* **1983**, *737*, 285.
(78) Neugebauer, J. M. *Meth. Enzymol.* **1990**, *182*, 239.
(79) Chattopadhyay, A.; Harikumar, K. G. *FEBS Lett.* **1996**, *391*, 199.
(80) Shobha, J.; Balasubramanian, D. *Proc. Indian Acad. Sci. (Chem. Sci.)* **1987**, *98*, 469.
(81) Dennis, K. J.; Luong, T.; Reshwan, M. L.; Minch, M. J. *J. Phys. Chem.* **1993**, *97*, 8328.
(82) Mukherjee, S.; Chattopadhyay, A. *Biochemistry* **1996**, *35*, 1311.
(83) Rajarathnam, K.; Hochman, J.; Schindler, M.; Ferguson-Miller, S. *Biochemistry* **1989**, *28*, 3168.
(84) Fery-Forgues, S; Fayet, J. P.; Lopez, A. *J. Photochem. Photobiol.* **1993**, *70*, 229.
(85) Stubbs, C. D.; Ho, C.; Slater, S. J. *J. Fluorescence* **1995**, *5*, 19.